IEEE Access
Multidisciplinary | Rapid Review | Open Access Journal

Received 24 February 2024, accepted 12 March 2024, date of publication 22 March 2024, date of current version 29 March 2024.

Digital Object Identifier 10.1109/ACCESS.2024.3380354

RESEARCH ARTICLE

Reconfigurable Intelligent Surface-Assisted NOMA With Coordinate Reflector Interleaving Under Rician Fading Channel

KRISMA ASMORO[1], I NYOMAN APRAZ RAMATRYANA[2], AND SOO YOUNG SHIN[1], (Senior Member, IEEE)

[1]Department of IT Convergence Engineering, Kumoh National Institute of Technology, Gumi 39177, South Korea
[2]Institute for Digital Communications, Friedrich-Alexander University Erlangen–Nürnberg, 91058 Erlangen, Germany

Corresponding author: Soo Young Shin (wdragon@kumoh.ac.kr)

This research was supported by the Ministry of Science and ICT (MSIT), Korea under the Information Technology Research Center (ITRC) support program (IITP-2024-RS-2023-00259061) supervised by the Institute for Information & Communications Technology Planning & Evaluation (IITP) and supported by the National Research Foundation of Korea (NRF) grant funded by the Korea government. (MSIT) (No. 2022R1A2B5B01001994).

ABSTRACT The concept of reconfigurable intelligent surface-assisted (RIS) for assisting non-orthogonal multiple access (NOMA) transmission, where the phases can be adjusted to decrease error rates and increase capacity, has been gaining popularity as a promising candidate for 6G communication and beyond. This paper considers RIS-NOMA downlink transmission under the Rician fading channel. A coordinate reflector interleaving (CRI) is proposed, where two groups of reflector elements are introduced, such as in-phase element and quadrature element groups. Therefore, it can reduce system complexity because of fewer successive interference cancellations (SIC) among users. As a result, a computer simulation shows that CRI-RIS-NOMA preserves a lower BER compared to conventional RIS-NOMA. Moreover, the superiority of CRI-RIS-NOMA over RIS-NOMA is that it can work at any power allocation for two users. This paper comprehensively studies theoretical derivation for 2 and 4 users to verify the computer-simulated BER. An upper-bound analysis of CRI-RIS-NOMA was also studied to observe the impact of RIS elements for high SNR cases.

INDEX TERMS Bit error rates (BER), coordinate reflector interleaving (CRI), non-orthogonal multiple access (NOMA), reconfigurable intelligent surfaces (RIS), rician fading.

I. INTRODUCTION

Wireless communications have advanced from first-generation to 6G, and the demand for reliable and high spectral efficiency is increasing. One main challenge to overcome beyond 6G communication is random channel and base station (BS) coverage. Reconfigurable intelligent surfaces (RIS) recently gained much interest due to its promising candidate to assist BS in beyond 6G communication [1]. RIS is a planar surface consisting of several reflecting elements that actively modify an incoming signal from BS and then reflect it to users [2]. In contrast with relay, RIS preserves a low-cost deployment because every element can be tuned independently to increase the signal-to-noise ratio (SNR) and consumes less energy [3]. The other benefit of RIS is that it can be integrated with existing multiple access techniques, providing high spectral efficiency and low error rates [4].

Numerous research studies have integrated RIS with existing multiple-access techniques, such as RIS-assisted non-orthogonal multiple access (NOMA). Specifically, power domain (PD) NOMA is a technique where multiple-user symbols are superimposed by adding specific power allocation (PA) with superposition coding (SC) [5]. Thus, the users with lower power allocation had to perform successive

The associate editor coordinating the review of this manuscript and approving it for publication was Ravi Kumar Gangwar.

interference cancellation (SIC) to obtain the information [6]. Therefore, NOMA can fulfill ever-increasing demands for high spectral efficiency performance and enormous bandwidth in 6G and potentially beyond [7]. Because of the NOMA benefit, RIS-NOMA is proposed to decrease error rates and increase spectral efficiency simultaneously [8]. However, RIS-NOMA is highly complex for many users due to its number of SIC processes. Moreover, with more than 2 users, the PA will become a complex problem.

The main objective of this paper is to reduce error rates that occur in RIS-NOMA communication. This paper introduces a novel coordinate reflector interleaving (CRI) to reduce SIC process in RIS-NOMA. In particular, CRI-based RIS-NOMA exploits signal space diversity (SSD) [9] by employing M-ary amplitude shift keying (MASK), which rotated as far as $\pi/4$. Furthermore, by exploiting the principle of signal separation in quadrature spatial modulation (QSM) [10], coordinate interleaving (CI) is applied on the transmitter and receiver to reduce detection complexity. In contrast with the existing constellation rotation NOMA (con-NOMA), which relies on SSD without RIS [11], [12].

A. RELATED WORKS

Based on the superiority of RIS to increase SNR for NOMA-based transmission, several works have been done to propose RIS-NOMA. Aside from RIS-NOMA to reduce BER for two users in [8], numerous algorithms have been proposed to enhance energy efficiency and sum rates. In [13], consider MISO-RIS-NOMA transmission and propose an algorithm to enhance energy efficiency by optimizing the BS and RIS precoding matrix. Numerous works to integrate RIS with NOMA technique have been done before to increase capacity have been done before. In [14], consider RIS single-input single-output (SISO) and proposed RIS beamforming for two NOMA users. In [15] improved the previous beamforming optimization by proposing a joint optimization of BS and RIS beamforming to maximize signal-to-interference-plus-noise ratio (SINR). User fairness is also considered in the works. In [16], consider a downlink RIS-NOMA scenario and propose user clustering to enhance energy efficiency. In [17] proposed a unique solution to enhance the sum rate for NOMA users. Consider a multiple-input single-output (MISO) BS-based transmission; near users are multiplexed with SDMA, while far users are served with RISs. In [18] propose a joint transmission coordinated multi-point (JT-CoMP) method to increase the ergodic capacity of the far users without reducing the capacity of the near users. In contrast with other previous work, [19] proposed capacity fairness for all NOMA users in SISO-RIS-NOMA and MIMO-RIS-NOMA.

According to SSD fundamentals in [9], several works to exploit constellation rotation have been done to reduce system complexity. In [20] proposed a constellation rotation for both near and far users in the NOMA downlink scenario. The main objective is to reduce BER and obtain an optimal rotation for two users. In [21] proposed a phase rotation for one of NOMA users. Then, SSD is applied to avoid overlapping signal constellation between users. Furthermore, in [22] extend the phase rotation system model for one of NOMA users. They proposed an algorithm to determine an optimal rotation value based on power allocation. Moreover, a close-form SER approximation was proposed for 4-QAM-based modulation. In [23], phase rotation NOMA is enhanced and applicable for generalized users to improve achievable data rates. Furthermore, an optimization rate is proposed to choose the suitable angle of the constellation rotation. Finally, in [24], an in-phase constellation rotation NOMA is proposed to enhance and reduce the BER of users and derive an SER approximation.

B. MOTIVATION AND CONTRIBUTION

Motivated by RIS and NOMA techniques, this study presents a novel CRI-RIS-NOMA to decrease BER. The CRI-RIS-NOMA can work under similar channel gain (resulting in similar power allocation).

In contrast with [8] and [19] which incorporate RIS and NOMA in the proposed system, this study proposed CRI-RIS-NOMA to reduce system complexity. In addition, this study derived analytical exact for 4 users NOMA with upper-bound approximation. Moreover, this study considers Rician fading scenario because Rayleigh fading is impractical in wireless telecommunication. This study contribution is summarized as follows:

- A novel technique CRI-RIS-NOMA is proposed to reduce number of SIC counts in the system. In contrast with traditional RIS-NOMA [8], BS will segregate cell users to utilize the in-phase or quadrature part of the signal constellation. Furthermore, by exploiting CI technique, users can detect the incoming signal with lower complexity.
- This study presents a complete derivation for 4 users CRI-RIS-NOMA with same modulation level. Based on derived Q-function, this study presents a novel analytical SER derivation for 2 and 4 user cases. In addition, this work considers Rician fading channel for generalized theoretical expression.
- Finally, to verify the exact analytical expression, this study presents an upper-bound approximation for a high transmit SNR case. Furthermore, this study analyzed the theoretical SER, which is proportional to high SNR and RIS elements.

This study considers Rician flat fading channel with given channel gain and Rician factor. Based on RIS capability to maximize SNR for cell users for 6G and beyond [25]. The proposed CRI-RIS-NOMA can assist BS transmission in sub-6GHz or THz communication. The derived analytical BER of this study is mainly focused on general case, regardless of the transmission band.

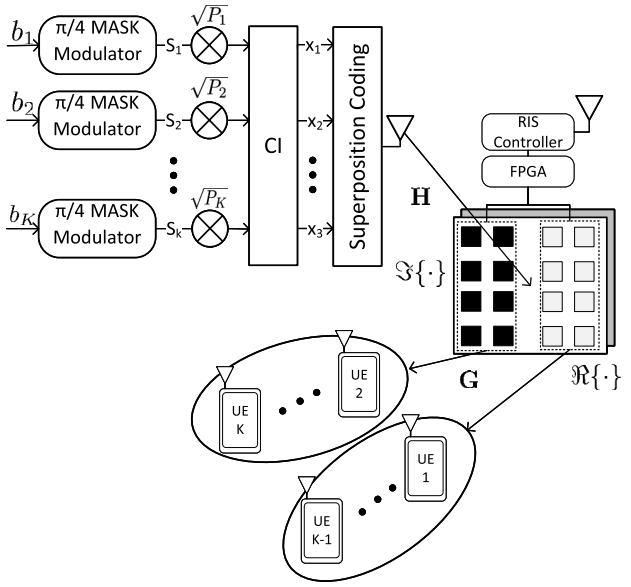

FIGURE 1. Block diagram of CRI-RIS-NOMA for generalized cell user.

C. PAPER ORGANIZATION

Firstly, the system model of CRI-RIS-NOMA is presented in Section II. The transmitter model and the example of CRI-RIS-NOMA are presented in Sub-Section II-A. The Rician channel model and user detector are presented in Sub-Section II-B The analytical BER of CRI-RIS-NOMA is derived in Section III. The theoretical approximation for 2 users case is derived in Sub-Section III-A and IV users case in Sub-section III-B. The numerical results are presented in Section IV to investigate the analytical and simulation results. Finally, the conclusion of this paper is presented in Section V.

II. SYSTEM MODEL

This study considers RIS-NOMA system and proposes CRI, as shown in Fig. 1. BS transmits information toward K user concurrently over Rician fading channel. It is presumed that BS had full knowledge of users' channel information.

A. TRANSMITTER MODEL

In CRI-RIS-NOMA, bits input are modulated with an M-ary amplitude shift keying (MASK) mapper. Contrary to conventional MASK, the constellation signal diagram is rotated as far as $\pi/4$ counter-clockwise. Suppose the user's index in the BS coverage is $k \in [1, 2, \cdots, K]$, then S_k is the modulated symbol of every user over $\pi/4$ MASK modulator. Therefore, it can be written as:

$$S_k = S_{kI} + S_{kQ}, \tag{1}$$

where S_{kI}, S_{kQ} are in-phase $\Re[\cdot]$ and quadrature $\Im[\cdot]$ components of S_k, respectively. The MASK modulation mapper is expressed as:

$$S_{kI} = S_{kQ} = (2m - 1 - M)\sqrt{\frac{3}{2M^2 - 2}}, \tag{2}$$

where m is the input symbol ($m \in [1, 2, \cdots, M]$) and M is the modulation order of the MASK modulator. Assuming there are two users in a cell ($K = 2$), the modulated symbols for users 1 and 2 are denoted by S_1 and S_2, respectively. The CI is applied on both users to obtain x_1 and x_2, it can be expressed as:

$$\begin{aligned} x_1 &= \sqrt{P_1}S_{1,I} + j\sqrt{P_2}S_{2,I}, \\ x_2 &= \sqrt{P_1}S_{1,Q} + j\sqrt{P_2}S_{2,Q}. \end{aligned} \tag{3}$$

In Eq. (3), P_k is the allocated transmitted power for a user k. P_k is $P_T\alpha_k$, where α_k is an PA coefficient for k^{th} user with its value $0 < \alpha_k < 1$, $\alpha_2 = 1 - \alpha_1$. P_T is the total transmit power on the BS. Thus, an allocated transmit power for user k is $0 < P_k < P_T$. Assuming $\alpha_2 \geq \alpha_1$ then, the channel gain of user 2 is lower or equal to user 1. The superposition signal from BS is denoted by $x = x_1 + x_2$ and x for user 1 and 2 is equal to $2x_1$. *Example: Utilizing Eq. (2), define* $\sqrt{P_k} = 1$, $S_1 = 1 + j$ *and* $S_2 = -1 - j$, *then CI is applied accordingly from Eq. (3). Therefore, the users symbol are* $x_1 = \Re\{S_1\} + \Re\{S_2\}$ *and* $x_2 = \Im\{S_1\} + \Im\{S_2\}$. *Thus,* $x_1 = 1 - j$ *and* $x_2 = 1 - j$ *are obtained and indicates that superposition coding* x *is equal to* $2x_1$.

In the proposed system, while $K = 2$, receivers are not required to do SIC to decode their information. This is because of the CI principle where user 1 symbol is mapped to a real component while user 2 is to an imaginary one. For a generalized number of users where $K > 2$, CI implementation for each user is divided into a user pairing group. Superposition users symbol x can be expressed as follows:

$$x_k = \begin{cases} \sqrt{P_k}s_{kI} + j\sqrt{P_{k+1}}s_{k+1,I} & \text{if } k \text{ is odd}, \\ \sqrt{P_{k-1}}s_{k-1,Q} + j\sqrt{P_k}s_{kQ} & \text{if } k \text{ is even}. \end{cases} \tag{4}$$

In Eq. (4), it can be seen that users are divided into an even group and an odd number group. Sum of x_k for $k = 1, 2, \cdots, K$ represents the transmitted base-band signal. It is important to take a note that $x_k = x_{k+1}$ for odd k^{th} user grouping, then $k = 1, 3, \cdots, K - 1$ and written as:

$$x = 2\sum_{\substack{k=1 \\ K \text{ is odd}}}^{K-1} x_k. \tag{5}$$

Then, for the generalized users' cases, a SIC corresponds within their grouping, and SIC is not performed for the user $(K - 1)^{th}$ and K user. Therefore, SIC process sequences are modeled as

$$\begin{aligned} &\text{SIC for} s_{K-1,I}, s_{K-3,I}, \ldots, s_{k+2,I} && \text{if } k \text{ is odd}, \\ &\text{SIC for} s_{K,I}, s_{K-2,I}, \ldots, s_{k+2,I} && \text{if } k \text{ is even}. \end{aligned} \tag{6}$$

B. CHANNEL MODEL AND DETECTOR

RIS contains a finite number of elements of N with i as an index of reflecting element, $i \in [1, 2, \cdots, N]$. The channel from single antenna BS to RIS is denoted by $\boldsymbol{H}$ while the

channel from RIS to cell users is denoted by $\boldsymbol{G}$. In this study, Rician fading channel is considered, and it can be written as:

$$G = \left(\underbrace{\sqrt{\frac{\varkappa}{2(1+\varkappa)}}}_{\boldsymbol{\mu}} G^{\text{LoS}} + \underbrace{\sqrt{\frac{1}{2(1+\varkappa)}}}_{\boldsymbol{\sigma}} G^{\text{NLoS}} \right), \quad (7)$$

where $\varkappa$ denotes Rician factor, the channel gain ratio of LoS and NLoS can be obtained from $\varkappa = \mu^2/\sigma^2$. In Eq. (7), $\mu_k \in \boldsymbol{\mu}$ denotes channel gain for LoS channel, whilst $\sigma_k \in \boldsymbol{\sigma}$ is channel gain for NLoS channel of user k. Furthermore, the received signal of user k can be expressed as:

$$y_k = H\boldsymbol{\Phi}G^{\text{T}}x + n = \left[\sum_{i=1}^{N} h_i e^{j\phi_i} g_{i,k}\right] x_k + n_k, \quad (8)$$

where $\left[H \in \mathbb{C}^{1\times N}, \boldsymbol{\Phi} \in \mathbb{C}^{N\times N}, G \in \mathbb{C}^{K\times N}\right]$. Additionally, n_k denotes an AWGN noise with mean 0 and variance N_0. The $\boldsymbol{\Phi}$ denotes an RIS phase shifter that is defined as:

$$\boldsymbol{\Phi} = \text{diag}\{\Lambda_1 e^{j\phi_1}, \cdots, \Lambda_i e^{j\phi_i}, \cdots, \Lambda_N e^{j\phi_N}\}, \quad (9)$$

where Λ_i is an RIS element magnitude ($|\boldsymbol{\Phi}| = 1$) and ϕ_i is a phase response of RIS elements ($\angle(\boldsymbol{\Phi})$). Assume h_i is channel from BS to i^{th} RIS element and the $g_{i,k}$ is channel from i^{th} RIS element to k^{th} user. Magnitude and channel phase of h_i and $g_{i,k}$ are denoted by $A_i e^{j\psi_i}$ and $\beta_{i,k} e^{j\theta_{i,k}}$, respectively. Therefore, a value of the RIS phase is defined as $\phi_i = \psi_i + \theta_{i,k}$. [14], [26].

Here, RIS elements are utilized to minimize channel phase. With given condition, the instantaneous SNR at receiver is written as:

$$\gamma_{ins\ k} = \frac{\sqrt{P_k}|\sum_{i=1}^{N} \Lambda_i A_i \beta_{i,k} e^{j(\phi_i - \psi_i - \theta_{i,k})}|^2}{N_0}. \quad (10)$$

On the receiver side, the maximum likelihood (ML) is performed to detect b_k. Therefore, it can be written as:

$$\hat{b}_k = \arg\min_{b_k} \left| y_k - \sqrt{P_k} \underbrace{\sum_{i=1}^{N} \left(h_i e^{j\phi_i} g_{i,k}\right) S_k}_{Z_k} \right|^2, \quad (11)$$

where $\boldsymbol{Z}_k$ is the channel vector of user k and $\hat{b}_k$ denotes a detected symbol.

III. PERFORMANCE ANALYSIS

A. 2 USERS CASE

The detection of two-user CRI-RIS is expressed with a maximum likelihood (ML) detector at a single-antenna receiver. Therefore, analytical symbol error rates (SER) over AWGN channel can be expressed as [27]:

$$P_k(e|\boldsymbol{Z}_k) = 2\frac{M-1}{M} Q\left(\sqrt{12\frac{\alpha_k|\Omega_k|^2}{M^2-1}\frac{P_T}{N_0}}\right), \quad (12)$$

where $|\Omega_k|^2$ is channel gain of user k, P_T is the total transmit power, and M is the modulation level. Here, $Q(\cdot)$ denotes an Q-function with $Q(x) = \frac{1}{\sqrt{2\pi}}\int_x^\infty \exp\left(-\frac{u^2}{2}\right) du$. The average analytical SER over Rician fading can be calculated by employing moment generating function (MGF) [28], and it is denoted by:

$$\mathcal{M}(j\omega) = \left(\frac{1}{1-2j\omega\sigma^2}\right)^{\frac{n}{2}} \exp\left(\frac{j\omega s^2}{1-2j\omega\sigma^2}\right), \quad (13)$$

where $j\omega$ is moment of MGF, s denotes mean, and σ^2 denotes variance. Further, we follow the summation of N Rician random variables. Following the central limit theorem (CLT), the channel gain of user k served with $N \gg 1$ RIS elements can be expressed as $N|\Omega_k|$. Based on the SNR in Eq. (10), the mean and variance of Rician random variable A_i and $\beta_{i,k}$ are written as follows:

$$VAR\{A_i\beta_{i,k}\} = \varepsilon_k = 2\sigma^2 + \mu^2 - \frac{\pi\sigma^2}{2}\mathcal{L}_{1/2}^2\left(-\frac{\mu^2}{2\sigma^2}\right), \quad (14a)$$

$$\mathbb{E}\{A_i\beta_{i,k}\} = \upsilon_k = \sqrt{\frac{\pi}{2}}\mathcal{L}_{1/2}\left(-\frac{\mu^2}{2\sigma^2}\right)\sigma, \quad (14b)$$

where $\mathcal{L}.(\cdot)$ denotes Laguerre polynomial. Given the mean and variance of Rician random variable, then MGF of Eq. (13) can be equivalently written as $\mathcal{M}(j\omega) = \left(\frac{1}{1-2j\omega\varepsilon_k}\right)^{\frac{n}{2}} \exp\left(\frac{j\omega\upsilon_k^2}{1-2j\omega\varepsilon_k}\right)$. Therefore, with the impact of Rician factor [29], the MGF of CRI-RIS-NOMA can be written as:

$$\mathcal{M}\left(-\frac{N\ell\gamma_k^P|\Omega_k|^2}{\sin^2\xi}\right) = \frac{(1+\varkappa)\sin^2\xi}{(1+\varkappa)\sin^2\xi + N\ell\bar{\gamma}_k^P\varepsilon_k^2} \times \exp\left(-\frac{\varkappa N^2\,\ell\bar{\gamma}_k^P\upsilon_k^2}{(1+\varkappa)\sin^2\xi + N\ell\bar{\gamma}_k^P\varepsilon_k^2}\right), \quad (15)$$

where $\bar{\gamma}_k^P = P_k/N_0$, $\ell = 3/(M^2-1)$ and $|\Omega_k|^2 = 1$. Finally, the analytical SER expression of the proposed system for 2 users ($|\Omega_k| \in [|\Omega_1|, |\Omega_2|]$) MASK can be written as:

$$\bar{P}_k^s = \frac{2(M-1)}{M\pi}\int_0^{\pi/2} \frac{(1+\varkappa)\sin^2\xi}{(1+\varkappa)\sin^2\xi + N\ell\bar{\gamma}_k^P|\Omega_k|^2\varepsilon_k^2} \times \exp\left(-\frac{\varkappa N^2\,\ell\bar{\gamma}_k^P|\Omega_k|^2\upsilon_k^2}{(1+\varkappa)\sin^2\xi + N\ell\bar{\gamma}_k^P|\Omega_k|^2\varepsilon_k^2}\right) d\xi. \quad (16)$$

B. 4 USERS CASE

For $K = 4$ case,[1] we can divide users who perform SIC ($c \in [1, 2]$) and non-SIC users as ($n \in [3, 4]$). Suppose decision boundary of ML detector with given received signal y_n for user n is denoted by $\Re\{\boldsymbol{y}_n\} < 0$, $\Re\{\boldsymbol{y}_n\} \geq 0$ and $\Im\{\boldsymbol{y}_n\} < 0$, $\Im\{\boldsymbol{y}_n\} \geq 0$. Therefore, the error probability of ML detector

[1] In this study, the proposed exact analytical method is derived until 4 users due to its complexity. For the analytical CRI-RIS-NOMA, generalized users are left for readers' interest.

under condition channel for all n users, $\mathbf{Z}_n = \sum_{i=1}^{N} h_i e^{j\phi_i} g_{i,n}$ can be written as:

$$P_n\left(e \mid \mathbf{Z}_n\right) = \frac{1}{2} P_r\left(\Re\{\boldsymbol{B}_n\} \geq \sqrt{\frac{P_T}{2}} L_A \mathbf{Z}_n \mathbf{Z}_n^{\mathbf{H}}\right) + \frac{1}{2} P_r\left(\Re\{\boldsymbol{B}_n\} \geq \sqrt{\frac{P_T}{2}} L_B \mathbf{Z}_n \mathbf{Z}_n^{\mathbf{H}}\right), \quad (17)$$

where L denotes a decision boundary based on power allocation with $L_A = \sqrt{\alpha_n} + \sqrt{\alpha_c}$ and $L_B = \sqrt{\alpha_n} - \sqrt{\alpha_c}$. $\Re\{\boldsymbol{B}_n\}$ denotes AWGN with zero mean and $N_0/2$ variance. Further, the BEP of users n in the form of a Q-function can be written as:

$$P_{n,\Re}(e|\,|\Omega_n|) = \frac{M-1}{M}\left[Q\left(\sqrt{12\frac{L_A^2|\Omega_n|^2}{M^2-1}\frac{P_T}{N_0}}\right) + Q\left(\sqrt{12\frac{L_B^2|\Omega_n|^2}{M^2-1}\frac{P_T}{N_0}}\right)\right]. \quad (18)$$

Consider ML decision rules and $\Im\{\boldsymbol{B}_n\}$, the error probability of user n is similar to Eq. (18). The error probability of it can be formulated as $P_n(e) = (P_{n,\Re}(e) + P_{n,\Im}(e))/2$. Finally, the MGF in Eq. (13) is utilized to estimate an SER of users n. Therefore, with given BEP in the form of Q-function in Eq. (18), it can be rewritten as follows:

$$\bar{P}_n^s = \frac{2(M-1)}{M\pi}\left(\int_0^{\pi/2} \mathcal{M}\left(-\frac{N\ell\gamma_n^A|\Omega_k|^2}{\sin^2\xi}\right) + \mathcal{M}\left(-\frac{N\ell\gamma_n^B|\Omega_k|^2}{\sin^2\xi}\right)\right), \quad (19)$$

where $\bar{\gamma}_n^A$ denotes $(\sqrt{\alpha_n} + \sqrt{\alpha_c})^2 P_T/N_0$, while $\bar{\gamma}_n^B$ denotes $(\sqrt{\alpha_n} - \sqrt{\alpha_c})^2 P_T/N_0$.

In contrast with user n, user c had to perform SIC. As a result, the analysis for user c can be divided by two conditions: BEP under the condition of detected symbol user n correctly and erroneously. Therefore, BEP for user c can be written as:

$$P_c(e) = P_c(e|\ correct_n) + P_c(e|\ error_n). \quad (20a)$$

Proposition. *The symbols of user n are presumed to be detected correctly and erroneously, further subtracted from the received signal at c. Therefore, BEP of user c can be written as in Eq. (20b), shown at the bottom of the page.*

Proof: See Appendix A for correct detection and Appendix B for incorrect detection of user n symbols. ■

Based on proposition Eq. (20a), the BEP of user c in the form of Q-function is obtained with $P_c(e) = (P_{c,\Re}(e) + P_{c,\Im}(e))/2$. Then, exact BEP of CRI-NOMA is expressed by (20b). Given BEP, to estimate $\bar{P}_n^s$, the MGF from Eq.(13) is utilized for transforming Eq. (20b) to SER over Rician fading channel. Then, the approximation of SER $\bar{P}_c^s$ can be written as Eq. (20c), shown at the bottom of the page, where $\bar{\gamma}_c^C$ denotes $(\sqrt{\alpha_c})^2$, $\bar{\gamma}_c^F$ denotes $(2\sqrt{\alpha_n} - \sqrt{\alpha_c})^2$, $\bar{\gamma}_c^G$ denotes $(2\sqrt{\alpha_n} + \sqrt{\alpha_c})^2$, and $\bar{\gamma}_n^E = \bar{\gamma}_n^A$; $\bar{\gamma}_n^D = \bar{\gamma}_n^B$.

C. SER UPPERBOUND ANALYSIS

This study derived and simulated an SER upper-bound theoretical approximation through computer simulation. Moreover, it analyses the impact of RIS elements number N and approximation for high transmit SNR.

To approximate upper-bound analysis, recalling Eq. (16), all $\xi = \pi/2$. Therefore, the upper bound expression $\bar{P}_k^u$ of the proposed system for two users is written as:

$$\bar{P}_k^s \leq \frac{2(M-1)}{M\pi}\frac{1+\varkappa}{1+\varkappa+N\varepsilon_k^2\ell\bar{\gamma}_k^P|\Omega_k|^2} \times \exp\left(-\frac{\varkappa N^2\ \upsilon_k^2\ell\bar{\gamma}_k^P|\Omega_k|^2}{1+\varkappa+N\varepsilon_k^2\ell\bar{\gamma}_k^P|\Omega_k|^2}\right). \quad (21)$$

Eq. (21) shows that the impact of Rician factor $\varkappa$ affects SER upper bound analysis. From the second term of exponent, the $\varkappa$ acts as a multiplier of N^2. Thus, it can be concluded that $\varkappa \to \infty$ then $\bar{P}_k^u \to \infty$ as well for LoS case. In contrast, with $\varkappa = 0$, the $\bar{P}_k^u$ is only affected by the power of N^2.

Based on the proposed upper bound results, with the assumption of $N\bar{\gamma}_k^P \gg 1$, the approximation of upper bound is proportional to:

$$\bar{P}_k^s \propto \exp\left(-\frac{\varkappa N^2\ \upsilon_k^2\ell\bar{\gamma}_k^P|\Omega_k|^2}{1+\varkappa+N\varepsilon_k^2\ell\bar{\gamma}_k^P|\Omega_k|^2}\right). \quad (22)$$

$$P_{c,\Re}(e) = \frac{M-1}{M}\left[2\times Q\left(\sqrt{12\frac{(\sqrt{\alpha_c})^2|\Omega_c|^2}{M^2-1}\frac{P_T}{N_0}}\right) + Q\left(\sqrt{12\frac{(\sqrt{\alpha_n}-\sqrt{\alpha_c})^2|\Omega_c|^2}{M^2-1}\frac{P_T}{N_0}}\right) - Q\left(\sqrt{12\frac{(\sqrt{\alpha_n}+\sqrt{\alpha_c})^2|\Omega_c|^2}{M^2-1}\frac{P_T}{N_0}}\right) - Q\left(\sqrt{12\frac{(2\sqrt{\alpha_n}-\sqrt{\alpha_c})^2|\Omega_c|^2}{M^2-1}\frac{P_T}{N_0}}\right) + Q\left(\sqrt{12\frac{(2\sqrt{\alpha_n}+\sqrt{\alpha_c})^2|\Omega_c|^2}{M^2-1}\frac{P_T}{N_0}}\right)\right]. \quad (20b)$$

$$\bar{P}_c^s = \frac{2(M-1)}{M\pi}\left(2\times\int_0^{\pi/2}\mathcal{M}\left(-\frac{N\ell\gamma_c^C|\Omega_c|^2}{\sin^2\xi}\right) + \mathcal{M}\left(-\frac{N\ell\gamma_c^D|\Omega_c|^2}{\sin^2\xi}\right) - \mathcal{M}\left(-\frac{N\ell\gamma_c^E|\Omega_c|^2}{\sin^2\xi}\right) - \mathcal{M}\left(-\frac{N\ell\gamma_c^F|\Omega_c|^2}{\sin^2\xi}\right) + \mathcal{M}\left(-\frac{N\ell\gamma_c^G|\Omega_c|^2}{\sin^2\xi}\right)\right), \quad (20c)$$

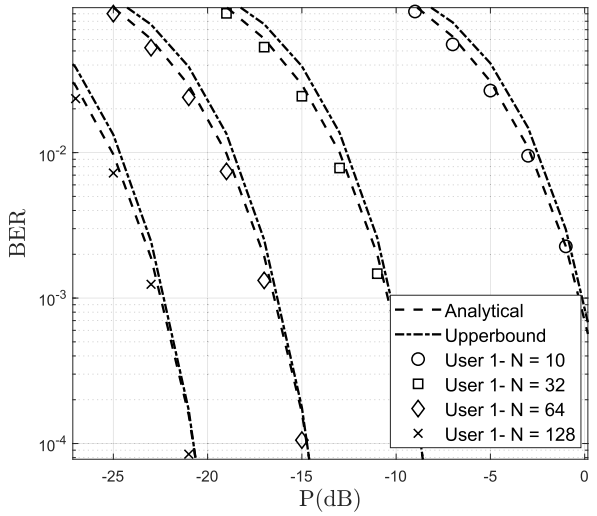

FIGURE 2. Simulation result ($K = 2$) of user 1 with the different number of elements and upper bound analysis.

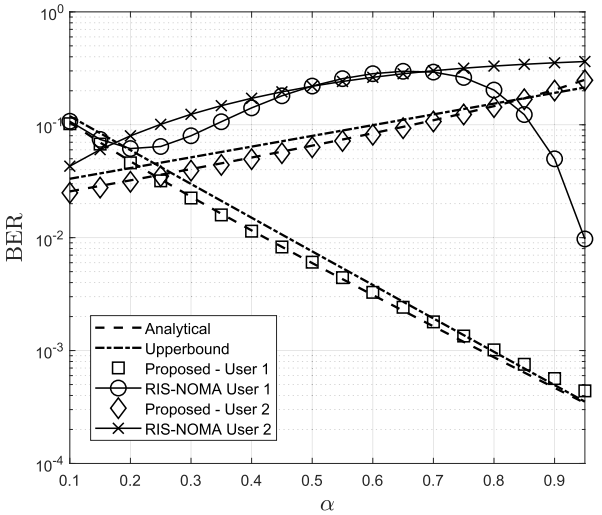

FIGURE 3. The simulation result of different α with same modulation $M = 4$ and transmit power $P = -6$dB.

Here, the impact of the number of RIS is exponentially increasing with the factor of N^2 and Ricean factor $\varkappa$. Therefore, it can be seen from Fig. 2 that the proposed system will achieve lower BER with the increasing element of N. In addition, Fig. 2 shows an upper bound result of the proposed system. It can be seen that the characteristics of upper bound analysis are closely tight with exact SER approximation as $\frac{P_T}{N_0} \rightarrow \infty$. A higher RIS element number N leads to a tight upper bound and exact analysis for low P_T.

IV. NUMERICAL RESULTS

This study compares CRI-RIS-NOMA BER performance to conventional 2 users RIS-NOMA in [8] and [19]. Then, given power allocation, this study extends 2 to 4 users to compare the proposed system's superiority to RIS-NOMA. Finally, SER performance results are validated with the exact and upper-bound analytical derived in the previous section. This study considers a different channel gain for cell users and follows the previous classical NOMA assumption in [8], [30], and [31]. Assuming user 1 is cell center user with strongest channel gain, then $K-1$ users will follow the rules $|\Omega_1|^2 = 0$, $|\Omega_2|^2 = |\Omega_1|^2 - X, \cdots, |\Omega_K|^2 = |\Omega_{K-1}|^2 - X$, with X being a -5 dB in value. Therefore, the channel gain of all users is defined as follows[2]: $|\Omega_1|^2 = 0$dB; $|\Omega_2|^2 = -5$dB; $|\Omega_3|^2 = -10$dB; $|\Omega_4|^2 = -15$dB;. In this study, the conversion of SER to BER is calculated as $\approx \text{SER}/log2(M)$ and $M = 4$.

Fig. 3 shows BER performance of the proposed system over different α_1, compared to RIS-NOMA. The transmit power is -6dB, $\varkappa = 7$dB, $N = 12$. Compared to RIS-NOMA, the proposed system can perform on every PA. The figure shows that for α is higher than 0.5, BER of RIS-NOMA user 2 stays above 10^{-1}. In addition, BER performance for user 1 keeps decreasing for a higher value of α.

[2]1 dB referred as 1 dBW which held $\approx$ 1.258 W (watts). To convert from logarithmic or dB to linear scale, this study employs $|\Omega_1|^2(\text{W}) = 10^{|\Omega_1|^2(dB)/10}$.

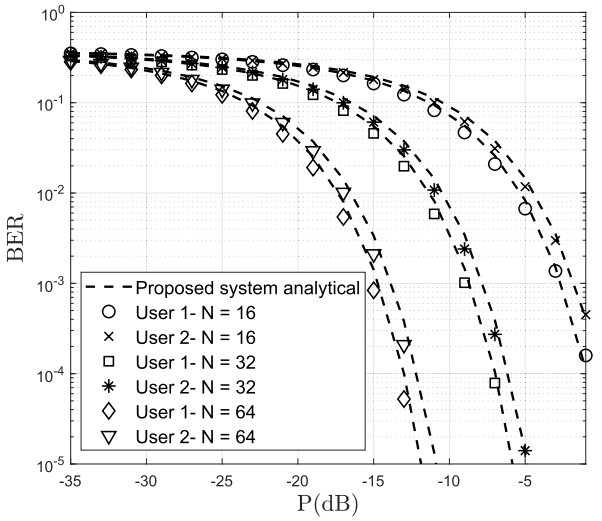

FIGURE 4. BER simulation and analytical result for different number of elements N with user 1 power allocation $\alpha_1 = 0.17$.

Fig. 4 shows BER performance of the proposed system over a different number of elements $N = [16, 32, 64]$. In addition, the parameter is set as follows: $\alpha_1 = 0.28$; $\varkappa = 3$dB. The figures show that BER is lower for more RIS elements. Targeting BER of User 2 below 10^{-3} is achieved with transmit power $P_T = -1$dB for $N = 16$, $P_T = -7$dB for $N = 32$, $P_T = -13$dB for $N = 32$.

In Fig. 5, we set the parameter as follows: $N = 64$; $\varkappa = 3$dB; α for a CRI-RIS user 1 to 4 is $\alpha = [2/52, 2/52, 24/52, 24/52]$; while for the NOMA users are $\alpha = [1/156, 5/156, 25/156, 125/156]$, respectively. As expected, The PA of CRI-RIS-NOMA for user 1 and user 2 can be set as the same because CRI-RIS-NOMA can work over different PAs. The figure shows clearly that

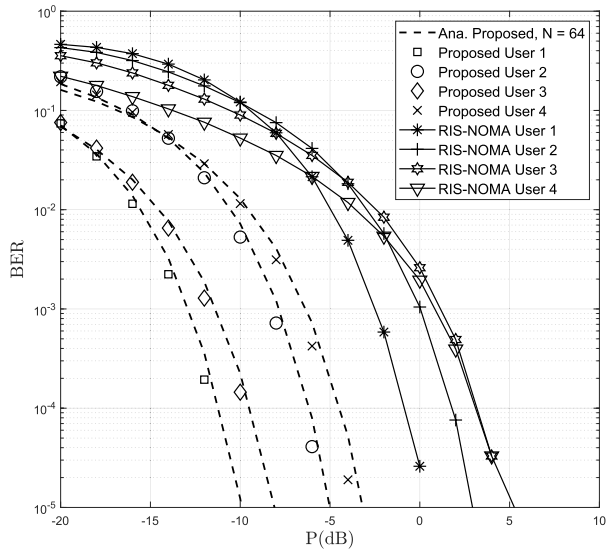

FIGURE 5. The result of generalized user proposed system ($N = 64$), compare to RIS-NOMA.

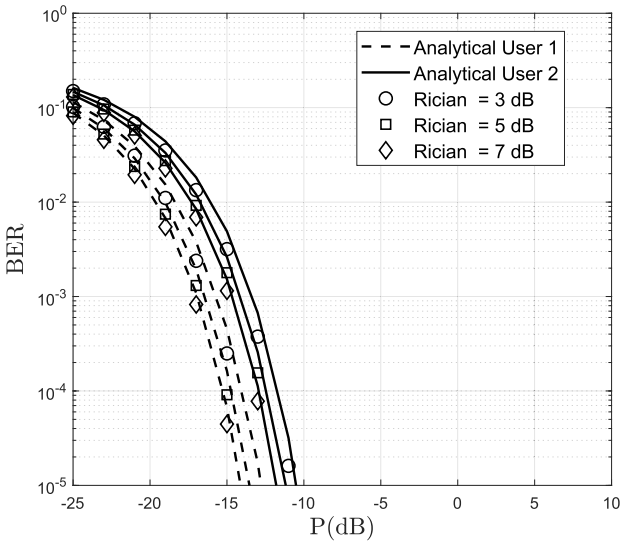

FIGURE 6. The BER result of different Rician factor κ with $N = 64$.

proposed system outperformed RIS-NOMA. Additionally, an impact of CI of real and imaginary components of the modulated signal makes the BER of User 3 near User 1, while User 4 is near User 2. Targeting BER at $\approx 10^{-4}$, user 1 CRI-RIS-NOMA can achieve it at $P_T = -12$dB, while RIS-NOMA at $P_T = 0$dB. User 2 CRI-RIS-NOMA achieve it at $P_T = -6$dB, RIS-NOMA at $P_T = 2$dB. User 3 CRI-RIS-NOMA achieve it at $P_T = -10$dB, RIS-NOMA at $P_T = 4$dB. User 4 CRI-RIS-NOMA achieve it at $P_T = -4$dB, RIS-NOMA at $P_T = 4$dB.

Fig. 6 shows result of different Rician factors with the same number of elements $N = 64$ and $\alpha = 0.35$. As expected, higher Rician factor $\varkappa$ leads to lower BER because of stronger LoS channel gain. However, the impact of higher κ Targeting BER under 10^{-4}, User 2 can achieve it with $P_T = -11$dB at $\varkappa = 3$dB, $P_T = -13$dB at $\varkappa = 5$dB and $P_T = -14$dB at $\varkappa = 7$dB.

V. CONCLUSION

This study proposes a novel CRI-RIS-NOMA to reduce SIC count. As a result, CRI-RIS-NOMA outperforms RIS-NOMA in terms of simulated BER. Furthermore, the proposed analytical BER validates simulated results for 2 and 4 users CRI-RIS-NOMA. Compared to conventional RIS-NOMA, CRI-RIS-NOMA exploits CI technique; thus, it gives a lower system complexity by reducing NOMA's SIC to half with several cell users. The trade-off of CRI-RIS-NOMA is that it has a relatively higher BER than RIS-aided orthogonal multiple access (RIS-OMA) due to power allocation for each user. As a gain, the proposed system has a higher sum rate than RIS-OMA. Further investigation for sub-6GHz or THz transmission with a sophisticated channel model (e.g., Saleh-Valenzuela model) appears essential for CRI-RIS-NOMA application in 6G communication. In addition, the future research direction is to integrate spatial modulation (SM) with CRI-RIS-NOMA to decrease system complexity even more.

APPENDIX A
BEP CORRECT DETECTION

In this case, conditional probability for user c on $\boldsymbol{B}_c$ includes the prior probability of correct detection of user n. Therefore, the conditional probability of user c, under condition symbol user n detected correctly can be written as:

$$\begin{aligned} &P_c\left(e|_{\text{correct }n,\Re\{\boldsymbol{B}_c\}}\right) \\ &= \frac{1}{2}P_r\left(\Re\{\boldsymbol{B}_c\} \geq -\sqrt{P_T}\left(\sqrt{a_n/2}+\sqrt{a_c/2}\right)\mathbf{Z}_c\mathbf{Z}_c^{\mathbf{H}}\right) \\ &\quad \times P_r\left(\Re\{\boldsymbol{B}_c\} < -\sqrt{P_T}\left(\sqrt{a_c/2}\right)\mathbf{Z}_c\mathbf{Z}_c^{\mathbf{H}}\right. \\ &\qquad \left.| \Re\{\boldsymbol{B}_c\} \geq -\sqrt{P_T}(\sqrt{a_n/2}+\sqrt{a_c/2})\mathbf{Z}_c\mathbf{Z}_c^{\mathbf{H}}\right) \\ &\quad + \frac{1}{2}P_r\left(\Re\{\boldsymbol{B}_c\} \geq -\sqrt{P_T}\left(\sqrt{a_n/2}-\sqrt{a_c/2}\right)\mathbf{Z}_c\mathbf{Z}_c^{\mathbf{H}}\right). \end{aligned} \tag{23}$$

To derive the error probability of user c with MASK modulation, conditional probability $Pr(x \mid y) = \frac{Pr(x \cap y)}{Pr(y)}$ is utilized. Furthermore, bit error probability (BEP) can be written as:

$$\begin{aligned} &P_{c,\Re}(e|\ correct_n) \\ &= \frac{M-1}{M}\left[2 \times Q\left(\sqrt{12\frac{(\sqrt{\alpha_c})^2|\Omega_c|^2}{M^2-1}\frac{P_T}{N_0}}\right)\right. \\ &\quad \left. - Q\left(\sqrt{12\frac{(\sqrt{\alpha_n}+\sqrt{\alpha_c})^2|\Omega_c|^2}{M^2-1}\frac{P_T}{N_0}}\right)\right]. \end{aligned} \tag{24}$$

The BEP of user c can be easily obtained by substitute $\Re\{\boldsymbol{B}_c\}$ with $\Im\{\boldsymbol{B}_c\}$, resulting in the same result. Furthermore, conditional BEP under condition symbol user n detected cor-

rectly can be written as $P_c(e|correct_n) = (P_{n,\Re}(e|correct_n) + P_{n,\Im}(e|correct_n))/2$. Thus, this is complete proof.

APPENDIX B
BEP ERROR DETECTION

In this case, conditional probability for user c on $\boldsymbol{B}_c$ includes the prior probability of incorrect detection of user n. Employing the decision boundary of ML, we can write the conditional probability of user c under condition symbol user n detected erroneously as:

$$\begin{aligned}
&P_c\left(e|_{\text{error }n,\Re\{\boldsymbol{B}_c\}}\right)\\
&= \frac{1}{2}P_r\left(\Re\{\boldsymbol{B}_c\} < -\sqrt{P_T}\left(\sqrt{a_n/2}+\sqrt{a_c/2}\right)\boldsymbol{Z}_c\boldsymbol{Z}_c^{\mathbf{H}}\right)\\
&\quad\times P_r\left(\Re\{\boldsymbol{B}_c\} < -\sqrt{P_T}\left(2\sqrt{a_n/2}+\sqrt{a_c/2}\right)\boldsymbol{Z}_c\boldsymbol{Z}_c^{\mathbf{H}}\right.\\
&\quad\left.|\ \Re\{\boldsymbol{B}_c\} < -\sqrt{P_T}\left(\sqrt{a_n/2}+\sqrt{a_c/2}\right)\boldsymbol{Z}_c\boldsymbol{Z}_c^{\mathbf{H}}\right)\\
&\quad+\frac{1}{2}P_r\left(\Re\{\boldsymbol{B}_c\} < -\sqrt{P_T}\left(\sqrt{a_n/2}-\sqrt{a_c/2}\right)\boldsymbol{Z}_c\boldsymbol{Z}_c^{\mathbf{H}}\right)\\
&\quad\times P_r\left(\Re\{\boldsymbol{B}_c\} \geq -\sqrt{P_T}\left(2\sqrt{a_n/2}-\sqrt{a_c/2}\right)\boldsymbol{Z}_c\boldsymbol{Z}_c^{\mathbf{H}}\right.\\
&\quad\left.|\ \Re\{\boldsymbol{B}_c\} < -\sqrt{P_T}\left(\sqrt{a_n/2}-\sqrt{a_c/2}\right)\boldsymbol{Z}_c\boldsymbol{Z}_c^{\mathbf{H}}\right) \qquad (25)
\end{aligned}$$

Furthermore, we employ similar conditional probability $Pr(x \mid y) = \frac{Pr(x\cap y)}{Pr(y)}$ to calculate BEP. Finally, we can write the Q-function of user c under the condition of incorrect detection of bit user n, is written as follows:

$$\begin{aligned}
&P_{c,\Re}(e|\ error_n)\\
&= \frac{M-1}{M}\left[Q\left(\sqrt{12\frac{(\sqrt{\alpha_n}-\sqrt{\alpha_c})^2|\Omega_c|^2}{M^2-1}\frac{P_T}{N_0}}\right)\right.\\
&\quad -Q\left(\sqrt{12\frac{(2\sqrt{\alpha_n}-\sqrt{\alpha_c})^2|\Omega_c|^2}{M^2-1}\frac{P_T}{N_0}}\right)\\
&\quad \left.+Q\left(\sqrt{12\frac{(2\sqrt{\alpha_n}+\sqrt{\alpha_c})^2|\Omega_c|^2}{M^2-1}\frac{P_T}{N_0}}\right)\right]. \qquad (26)
\end{aligned}$$

Furthermore, conditional BEP under condition symbol user n detected incorrectly can be written as $P_c(e|error_n) = (P_{n,\Re}(e|error_n) + P_{n,\Im}(e|error_n))/2$. The proof is completed.

REFERENCES

[1] Q. Wu and R. Zhang, "Towards smart and reconfigurable environment: Intelligent reflecting surface aided wireless network," *IEEE Commun. Mag.*, vol. 58, no. 1, pp. 106–112, Jan. 2020.

[2] E. Basar, "Transmission through large intelligent surfaces: A new frontier in wireless communications," in *Proc. Eur. Conf. Netw. Commun. (EuCNC)*, Jun. 2019, pp. 112–117.

[3] M. Di Renzo, K. Ntontin, J. Song, F. H. Danufane, X. Qian, F. Lazarakis, J. De Rosny, D.-T. Phan-Huy, O. Simeone, R. Zhang, M. Debbah, G. Lerosey, M. Fink, S. Tretyakov, and S. Shamai (Shitz), "Reconfigurable intelligent surfaces vs. Relaying: Differences, similarities, and performance comparison," *IEEE Open J. Commun. Soc.*, vol. 1, pp. 798–807, 2020.

[4] E. Basar, M. Di Renzo, J. De Rosny, M. Debbah, M.-S. Alouini, and R. Zhang, "Wireless communications through reconfigurable intelligent surfaces," *IEEE Access*, vol. 7, pp. 116753–116773, 2019.

[5] Z. Ding, X. Lei, G. K. Karagiannidis, R. Schober, J. Yuan, and V. K. Bhargava, "A survey on non-orthogonal multiple access for 5G networks: Research challenges and future trends," *IEEE J. Sel. Areas Commun.*, vol. 35, no. 10, pp. 2181–2195, Oct. 2017.

[6] B. Selim, M. S. Alam, G. Kaddoum, and B. L. Agba, "Effect of impulsive noise on uplink NOMA systems," *IEEE Trans. Veh. Technol.*, vol. 69, no. 3, pp. 3454–3458, Mar. 2020.

[7] S. M. R. Islam, N. Avazov, O. A. Dobre, and K.-S. Kwak, "Power-domain non-orthogonal multiple access (NOMA) in 5G systems: Potentials and challenges," *IEEE Commun. Surveys Tuts.*, vol. 19, no. 2, pp. 721–742, 2nd Quart., 2017.

[8] V. C. Thirumavalavan and T. S. Jayaraman, "BER analysis of reconfigurable intelligent surface assisted downlink power domain NOMA system," in *Proc. Int. Conf. Commun. Syst. Netw. (COMSNETS)*, Jan. 2020, pp. 519–522.

[9] J. Boutros and E. Viterbo, "Signal space diversity: A power- and bandwidth-efficient diversity technique for the Rayleigh fading channel," *IEEE Trans. Inf. Theory*, vol. 44, no. 4, pp. 1453–1467, Jul. 1998.

[10] R. Mesleh, S. S. Ikki, and H. M. Aggoune, "Quadrature spatial modulation," *IEEE Trans. Veh. Technol.*, vol. 64, no. 6, pp. 2738–2742, Jun. 2015.

[11] N. Ye, A. Wang, X. Li, W. Liu, X. Hou, and H. Yu, "On constellation rotation of NOMA with SIC receiver," *IEEE Commun. Lett.*, vol. 22, no. 3, pp. 514–517, Mar. 2018.

[12] F. Huang, J. Yang, Z. Si, K. Niu, Z. He, and C. Dong, "The optimization of constellation rotation on the multi-user superposition modulation system," in *Proc. 3rd IEEE Int. Conf. Comput. Commun. (ICCC)*, Dec. 2017, pp. 41–45.

[13] X. Liu, Y. Liu, Y. Chen, and H. V. Poor, "RIS enhanced massive non-orthogonal multiple access networks: Deployment and passive beamforming design," *IEEE J. Sel. Areas Commun.*, vol. 39, no. 4, pp. 1057–1071, Apr. 2021.

[14] T. Hou, Y. Liu, Z. Song, X. Sun, Y. Chen, and L. Hanzo, "Reconfigurable intelligent surface aided NOMA networks," *IEEE J. Sel. Areas Commun.*, vol. 38, no. 11, pp. 2575–2588, Nov. 2020.

[15] G. Yang, X. Xu, and Y.-C. Liang, "Intelligent reflecting surface assisted non-orthogonal multiple access," in *Proc. IEEE Wireless Commun. Netw. Conf. (WCNC)*, May 2020, pp. 1–6.

[16] M. Zhang, M. Chen, Z. Yang, H. Asgari, and M. Shikh-Bahaei, "Joint user clustering and passive beamforming for downlink NOMA system with reconfigurable intelligent surface," in *Proc. IEEE 31st Annu. Int. Symp. Pers., Indoor Mobile Radio Commun.*, Aug. 2020, pp. 1–6.

[17] Z. Ding and H. V. Poor, "A simple design of IRS-NOMA transmission," *IEEE Commun. Lett.*, vol. 24, no. 5, pp. 1119–1123, May 2020.

[18] M. Elhattab, M.-A. Arfaoui, C. Assi, and A. Ghrayeb, "Reconfigurable intelligent surface assisted coordinated multipoint in downlink NOMA networks," *IEEE Commun. Lett.*, vol. 25, no. 2, pp. 632–636, Feb. 2021.

[19] G. Yang, X. Xu, Y.-C. Liang, and M. D. Renzo, "Reconfigurable intelligent surface-assisted non-orthogonal multiple access," *IEEE Trans. Wireless Commun.*, vol. 20, no. 5, pp. 3137–3151, May 2021.

[20] J. Zhang, X. Wang, T. Hasegawa, and T. Kubo, "Downlink non-orthogonal multiple access (NOMA) constellation rotation," in *Proc. IEEE 84th Veh. Technol. Conf. (VTC-Fall)*, Sep. 2016, pp. 1–5.

[21] Y. Chang and K. Fukawa, "Non-orthogonal multiple access with phase rotation employing joint MUD and SIC," in *Proc. IEEE 87th Veh. Technol. Conf. (VTC Spring)*, Jun. 2018, pp. 1–5.

[22] B. K. Ng and C.-T. Lam, "Joint power and modulation optimization in two-user non-orthogonal multiple access channels: A minimum error probability approach," *IEEE Trans. Veh. Technol.*, vol. 67, no. 11, pp. 10693–10703, Nov. 2018.

[23] A. Chauhan and A. Jaiswal, "Non-orthogonal multiple access: A constellation domain multiplexing approach," in *Proc. IEEE 31st Annu. Int. Symp. Pers., Indoor Mobile Radio Commun.*, Aug. 2020, pp. 1–6.

[24] H. Y. Lee and S. Y. Shin, "A novel user grouping in phase rotation based downlink NOMA," *IEEE Access*, vol. 10, pp. 27211–27222, 2022.

[25] M. Alsabah, M. A. Naser, B. M. Mahmmod, S. H. Abdulhussain, M. R. Eissa, A. Al-Baidhani, N. K. Noordin, S. M. Sait, K. A. Al-Utaibi, and F. Hashim, "6G wireless communications networks: A comprehensive survey," *IEEE Access*, vol. 9, pp. 148191–148243, 2021.

[26] M. Jian, G. C. Alexandropoulos, E. Basar, C. Huang, R. Liu, Y. Liu, and C. Yuen, "Reconfigurable intelligent surfaces for wireless communications: Overview of hardware designs, channel models, and estimation techniques," *Intell. Converged Netw.*, vol. 3, no. 1, pp. 1–32, Mar. 2022.
[27] M. K. Simon and M.-S. Alouini, *Digital Communication Over Fading Channels*, vol. 95. Hoboken, NJ, USA: Wiley, 2005.
[28] J. G. Proakis, *Digital Communications*, 5th ed. New York, NY, USA: McGraw-Hill, 2007.
[29] A. Goldsmith, *Wireless Communications*. Cambridge, U.K.: Cambridge Univ. Press, 2005.
[30] J. Cui, Z. Ding, and P. Fan, "A novel power allocation scheme under outage constraints in NOMA systems," *IEEE Signal Process. Lett.*, vol. 23, no. 9, pp. 1226–1230, Sep. 2016.
[31] Y. Zhao, J. Hu, Z. Ding, and K. Yang, "Joint interleaver and modulation design for multi-user SWIPT-NOMA," *IEEE Trans. Commun.*, vol. 67, no. 10, pp. 7288–7301, Oct. 2019.

KRISMA ASMORO received the bachelor's degree in telecommunication engineering from Telkom University, Indonesia, in 2018. He is currently pursuing the integrated master's and Ph.D. degree with the Department of IT Convergence Engineering, Kumoh National Institute of Technology, South Korea. His research interests include next-generation wireless technology, analysis of bit error rate (BER), capacity analysis, non-orthogonal multiple access (NOMA), multiple-input multiple-output (MIMO), reconfigurable intelligent surfaces (RIS), and spatial modulation (SM).

I NYOMAN APRAZ RAMATRYANA received the bachelor's degree in telecommunication engineering and the master's degree in electrical and telecommunication engineering from the Telkom Institute of Technology (currently known as Telkom University), Indonesia, in 2010 and 2014, respectively, and the Ph.D. degree in IT convergence engineering from the Kumoh National Institute of Technology, South Korea, in 2023. His research interests include signal processing, artificial intelligence (AI), wireless communications, computer vision, random access (RA), raptor coding, non-orthogonal multiple access (NOMA), multiple-input multiple-output (MIMO) antenna, compressed imaging, medical imaging, and deep learning (DL).

SOO YOUNG SHIN (Senior Member, IEEE) received the B.S., M.S., and Ph.D. degrees in electrical engineering and computer science from Seoul National University, South Korea, in 1999, 2001, and 2006, respectively. He was a Visiting Scholar with the FUN Laboratory, University of Washington, USA, from July 2006 to June 2007. He was with the WiMAX Design Laboratory, Samsung Electronics, for three years. He has been an Associate Professor with the School of Electronics, Kumoh National Institute of Technology, since September 2010. His research interests include wireless LAN, WPAN, WBAN, wireless mesh networks, sensor networks, coexistence among wireless networks, industrial and military networks, cognitive radio networks, and next-generation mobile wireless broadband networks.